

Monodisperse SiO₂ Microspheres with Large Specific Surface Area: Preparation and Particle Size Control

Shengkai LI¹, Xianjin XU², Wei LI¹, Lei WANG^{1*}, Haijin NING^{2*}, Shengliang ZHONG^{1*}

1. Research Center for Ultrafine Powder Materials, College of Chemistry and Chemical Engineering, Jiangxi Normal University, Nanchang 330022, China

2. Jiangxi KingPowder New Material Co., Ltd., Ganzhou 341003, China

*Corresponding authors: Lei WANG, Haijin NING, E-mail: slzhong@jxnu.edu.cn (S. L. Zhong)

Abstract:

Monodisperse SiO₂ microspheres have found applications in catalysis, drug delivery, coatings, cosmetics, optical sensing and plastics. The particle size of monodisperse SiO₂ microspheres is closely related to its application. In this paper, monodisperse SiO₂ microspheres with tunable diameter were successfully synthesized using cetyltrimethylammonium bromide (CTAB) as template. The monodisperse SiO₂ microspheres with diameters ranging from 200 nm to 3 μm were obtained by controlling the concentration of CTAB, tetraethyl orthosilicate (TEOS), diethanolamine (DEA) and reaction temperature. The BET surface area could reach 835 m² g⁻¹ and mean pore diameter was 2.3 nm. The formation mechanism of monodisperse SiO₂ microspheres was investigated.

Keywords: Monodisperse; SiO₂ microspheres; template method

1 Introduction

For the past few years, the superior performance of nanomaterials has received extensive attention from scholars. Monodisperse mesoporous SiO₂ microspheres have been widely used in catalysis^[1-5], drug loading^[6-8], coatings^[9-10], optical sensing^[11], plastics and other fields by virtue of their large specific surface area, good biocompatibility, stable physical and chemical properties, and easy functionalization of surface hydroxyl groups^[12].

As we all know, the particle size of monodisperse SiO₂ microspheres plays a decisive role in their application. For example, nanoscale monodisperse SiO₂ microspheres are widely used in biopharmaceuticals^[13], and micron-sized monodisperse SiO₂ microspheres are mostly used in cosmetics, coatings and other fields^[14-17]. Sol-gel method is the most widely used method for preparing SiO₂ particles^[18]. However, the size of SiO₂ spheres is less than 900 nm and can only be regulated between 10-500 nm. Although seed-mediated growth method can be used to prepare SiO₂ microspheres with a wider range of particle size, this reaction requires strict control of the proportion of various raw materials, as well as the addition rate of tetraethyl orthosilicate, stirring rate, reaction time, and other factors. The preparation of SiO₂ microspheres by a multi-step synthesis method is complicated and time-consuming. It

is easy to cause agglomeration or multiple nucleation during the growth of particles. Lei and his team used a modified sol-gel method to synthesize SiO₂ microspheres with particle sizes ranging from 1 μm to 3 μm^[19]. Monodisperse SiO₂ was prepared by a two-phase reaction. The monodisperse SiO₂ microspheres with core-shell structure were obtained by controlling the stirring speed, and specific surface area reached 233 m² g⁻¹^[20]. To extend the application of monodisperse SiO₂ microspheres in different fields, it is still a great challenge to prepare monodisperse SiO₂ microspheres with a wide particle size range and large specific surface area.

In this work, using cetyltrimethylammonium bromide (CTAB) as a template and diethanolamine (DEA) as a catalyst, monodisperse SiO₂ microspheres with particle sizes ranging from 200 nm to 3 μm were successfully synthesized and the effects of different reaction conditions to the morphology of the prepared monodisperse SiO₂ microspheres were studied and discussed.

2 Experimental section

2.1 Materials

DEA (99 %) and ethanol (99 %) were purchased from Damao Chemical Reagent Company (Tianjin, China). tetraethyl orthosilicate (TEOS, analytical grade) and CTAB (99 %) were obtained from

Aladdin Reagent Company (Shanghai, China). Deionized water was used in all experiments. All chemicals were used as received without purification.

2.2 Preparation of monodisperse SiO₂ microspheres

In a typical experiment, 0.08 g CTAB was dissolved in 15 mL water under stirring in a beaker. The obtained clear solution was heated to 30 °C in water bath. 15.0 mL TEOS (0.1 mol/L) was dropped into the above solution under stirring. And then, 2.0 mL DEA (0.1 mol/L) was slowly dropped into the above mixture under stirring. After stirring for 30 minutes, the mixture was kept under static conditions for 24 hours. The resulting monodisperse SiO₂ microspheres (sample 1) were separated by centrifuging and washed with ethanol twice and distilled water once and then dried in an oven at 60 °C. In order to eliminate the organic residues, the obtained products were thermal treated at 550 °C for 2 h in the air.

2.3 Characterization

The morphologies of the products were observed by a SEM equipped with an EDS (Hitachi, S-3400N). The nitrogen adsorption and desorption isotherms were measured on a BELSORP-mini II apparatus. The pore size and the pore diameter distributions were derived from the desorption branches of the isotherm with the Barrett-Joyner-Halenda (BJH) model. X-ray diffraction (XRD) patterns were collected using a Rigaku/Max-3A X-ray diffractometer with Cu-K α radiation ($\lambda = 1.54178$ Å) at a voltage of 30 kV and a current of 10 mA. ATA-50 thermal analyzer was used to record the TG curve at a

heating rate of 10 °C min⁻¹ from room temperature to 800 °C under an air atmosphere.

3 Results and discussion

3.1 Characterization of the typical product

SEM was carried out to observe the size and morphology of the synthesized sample 1. Figure 1 shows that the sample is composed of a large number of spheres with smooth surface and uniform particle size. Figure 2 is the energy spectrum of the sample. In order to further analyze the sample composition, XRD pattern of sample 1 is shown in Figure 3. The diffraction peak centered at 22° indicates that the obtained sample is amorphous structure SiO₂^[21]. Figure 4 shows the thermogravimetric spectrum of the prepared sample. It can be seen from the thermogravimetric curve of the sample that the first weight loss is between 40 and 200 °C, mainly due to the desorption process of water molecules adsorbed on the surface of the silica microspheres. The second weight loss is between 200 and 550 °C, presumably caused by the decomposition of surfactants and some organic substances in the sample, and the two weight loss rates are about 25%. Figure 5 shows a type I isotherm implying the existence of mesoporous, which is confirmed by the pore diameter distribution curve. Sample 1 has a specific surface area of 835 m² g⁻¹ and the mean pore diameter is 2.3 nm. From the above characterization, it can be seen that Sample 1 is a monodisperse silica microsphere with high purity and amorphous structure.

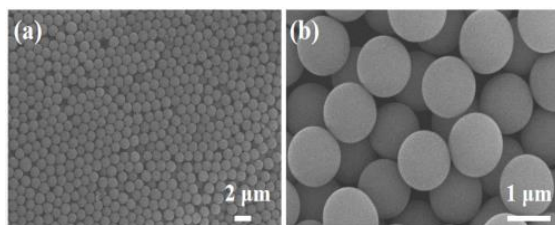


Figure 1 SEM images of sample 1

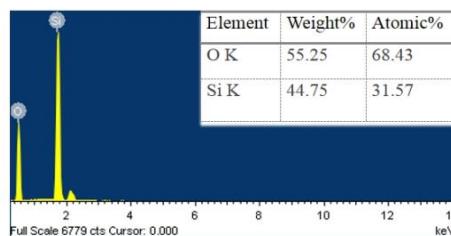


Figure 2 EDX spectrum of sample 1

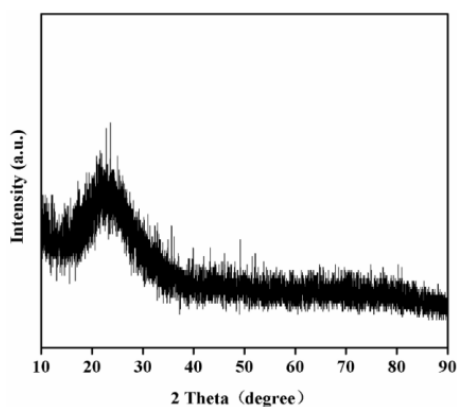


Figure 3 PXRD patterns of sample 1

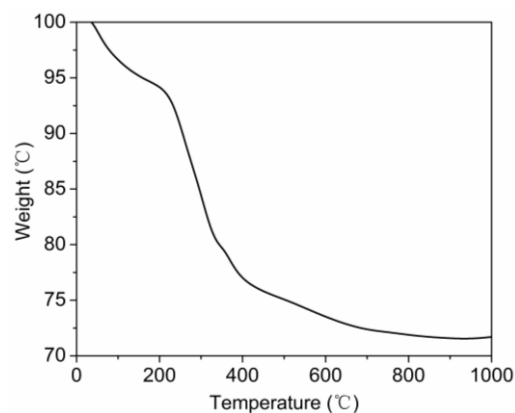


Figure 4 TG curve of the silica microspheres

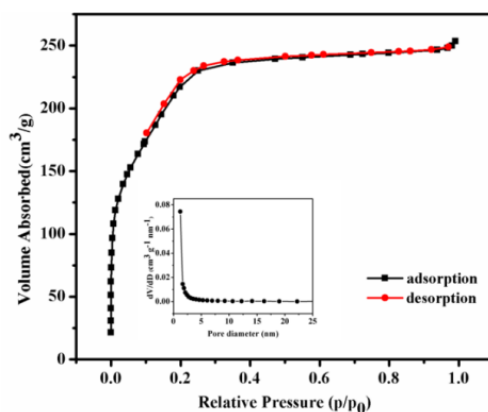


Figure 5 Nitrogen adsorption-desorption isotherms of sample 1 and the corresponding BJH pore size distribution curves

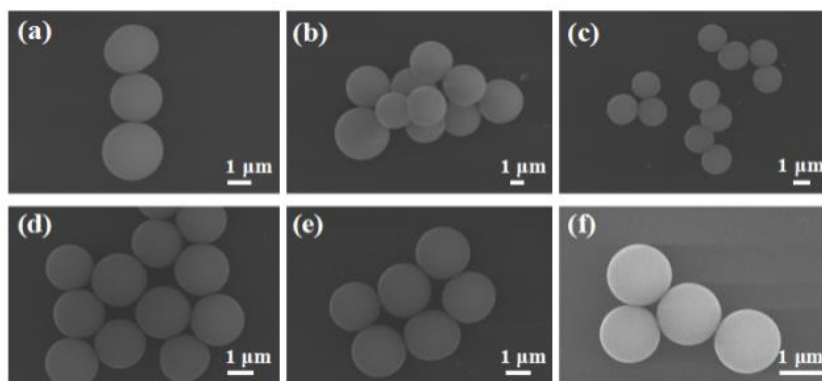


Figure 6 SEM images of SiO₂ particles obtained with different amount of CTAB in the solution: (a) 0.01 g, (b) 0.02 g, (c) 0.03 g, (d) 0.05 g, (e) 0.06 g, (f) 0.08 g

3.2 Effect of the CTAB on particle size and morphology

In the absence of CTAB as a template, no precipitation was observed in the solution, because the TEOS cannot undergo hydrolytic polycondensation. When the concentration of CTAB is low, the size of SiO₂ microspheres is uneven and the sphericity is not good, because low concentration of CTAB leads to the formation of very large micelles which is called worm-like micelles. When the concentration is greater than the critical micelle concentration, the shape of the

micelles is usually spherical [22-23]. In a typical experiment, at the same concentration of TEOS, the particle size of the monodisperse SiO₂ microspheres gradually decreases from 2.28 μm to 1.53 μm with the increase of CTAB (Figure 6), the particle size of the monodisperse SiO₂ microspheres gradually decreases to the similar size. Finally, the size of the SiO₂ microspheres was uniform and spherical. Figure 7 shows the size of the monodisperse SiO₂ microspheres, the corresponding particle sizes are 2.28, 2.05, 1.70, 1.80, 1.70, 1.53 μm.

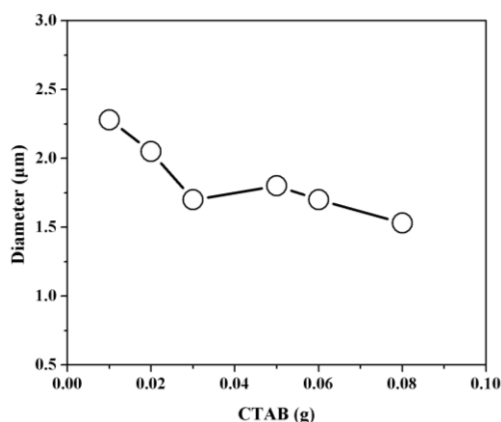


Figure 7 Effect of the amount of CTAB in the solution on the particle diameter

3.3 Effect of DEA on particle size

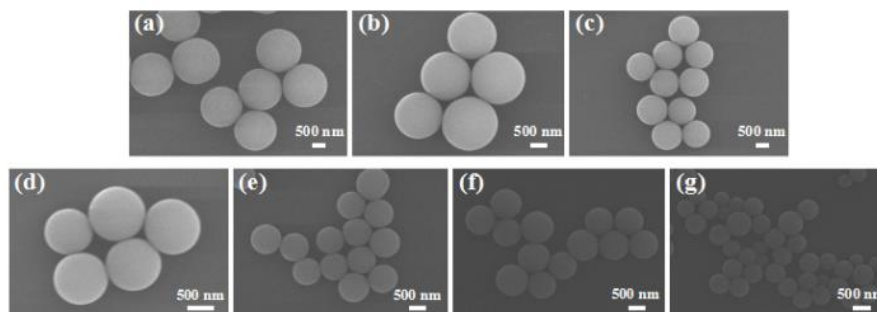


Figure 8 SEM images of SiO₂ particles obtained with different amount of DEA in the solution: (a) 1 mL, (b) 2 mL, (c) 3 mL, (d) 4 mL, (e) 5 mL, (f) 7 mL, (g) 9 mL

It can be seen from the Figure 8 that the particle size of the monodisperse SiO₂ microspheres gradually decreases from 1.70 μm to 0.55 μm with the increase of DEA. This is thought to be caused by the increasing of the hydrolysis rate of TEOS with the increase of DEA concentration, and thus resulting in the formation of SiO₂ core particles are formed in the early stage. At the same time, the DEA has the dual nature of ammonia and

alcohol and it partially ionizes in water, which effectively controls the alkaline environment of the system. The hydroxyl group in the molecule of DEA can also be complexed with the silicon hydroxyl group to terminate the self-condensation of the TEOS [24]. Figure 9 shows the size of monodisperse SiO₂ microspheres, the corresponding particle size is 1.70, 1.53, 1.16, 1.03, 0.82, 0.76, 0.55 μm, respectively.

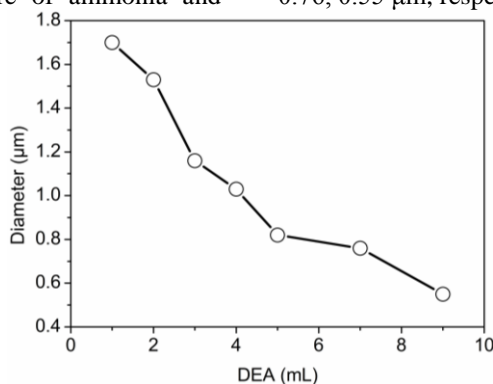


Figure 9 Effect of the DEA on the particle diameter

3.4 Effect of the TEOS on the particle size

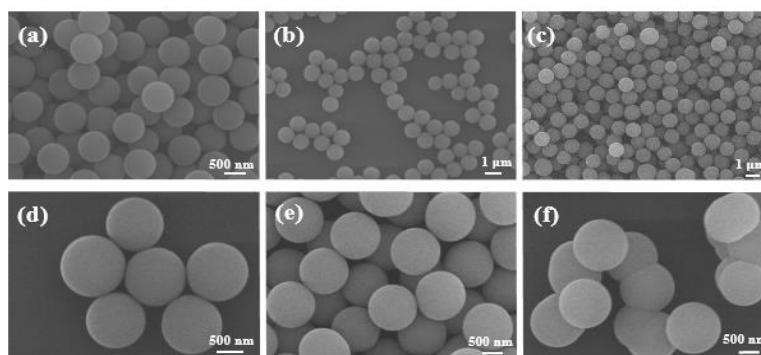


Figure 10 SEM images of SiO₂ particles obtained with different amount of TEOS in the solution: (a) 0.01 mol/L, (b) 0.05 mol/L, (c) 0.1 mol/L, (d) 0.15 mol/L, (e) 0.2 mol/L, (f) 0.3 mol/L

It can be seen from the Figure 10 that the particle size of the monodisperse SiO₂ microspheres increases gradually from 0.75 μm to 1.34 μm with the increase of the concentration of

TEOS. However, too high concentration of TEOS destabilizes the reaction system, leading to the adhesion of SiO₂ microspheres [25-26]. The conclusion is that with the

increase of TEOS, the particle size of SiO₂ microspheres increases and the output is improved. Figure 11 shows the

size of monodisperse SiO₂ microspheres, the corresponding particle size is 0.75, 1.07, 1.13, 1.16, 1.18, 1.34 μm.

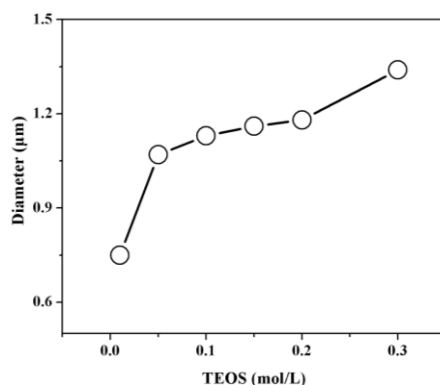


Figure 11 Effect of the TEOS on the particle diameter

3.5 Effect of temperature on the particle size

Experiments were carried out at different temperatures to investigate the effect of temperature on the formation of SiO₂ spheres. It was found that the reaction at low temperature was slow under the condition of equal DEA. With the increase of temperature, precipitation time is shortened, and precipitation occurs immediately at 60 °C. It can be seen from the Figure 12 that the particle size of the monodisperse SiO₂ microspheres decreases with the increase of temperature. At the same concentration of

TEOS, due to the slow hydrolysis rate of TEOS at low temperature, the formation of small particles of silicic acid nuclei is less, and the main reaction is polycondensation, which leads to the growth of SiO₂ microspheres. When the temperature is high, the hydrolysis rate of TEOS is accelerated. In the early stage, a large amount of TEOS is consumed to form a large number of small nucleating particles. In the later stage, smaller microspheres are formed [27]. As shown in Figure 13, the corresponding particle size is 1.53, 1.25, 1.13, 0.91, 0.87, 0.25 μm.

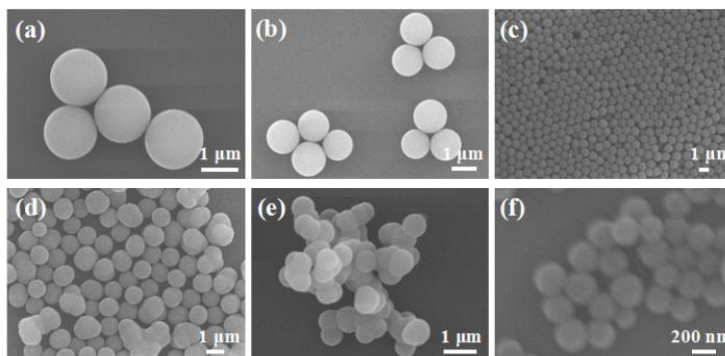


Figure 12 SEM images of SiO₂ particles obtained at different temperatures: (a) 5 °C, (b) 20 °C, (c) 30 °C, (d) 40 °C, (e) 50 °C, (f) 60 °C

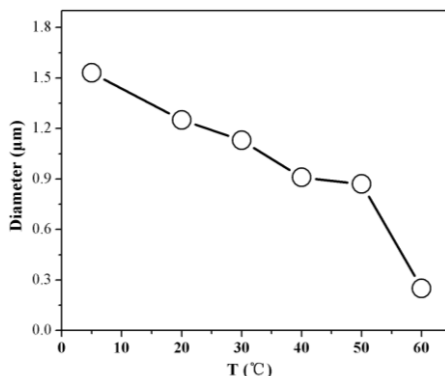


Figure 13 Effect of temperature on the particle diameter

4 Conclusions

Monodisperse SiO₂ microspheres with diameter from 200 nm to 3 μm are synthesized successfully by a template method, and BET surface area could reach 835 m² g⁻¹, mean pore diameter was 2.3 nm. The particle size range of the preparation of monodisperse SiO₂ microspheres was expanded, with the increase of CTAB concentration, the role of template causes SiO₂ microspheres to change from non-spherical to spherical and particle size of SiO₂ microspheres gradually decreased and remained unchanged. The sphericity and dispersion of SiO₂ microspheres gradually increased. With increase of DEA or temperature, the hydrolysis rate of TEOS is increased, more silicic acid nucleus particles are formed in the early stage, leading to the formation of smaller SiO₂ microspheres. The modest increase of TEOS concentration contributes to SiO₂ microspheres growth.

Acknowledgements: This work was supported by Jiangxi Provincial Department of Science and Technology (Nos. 20192BBEL50017 and 20202ACBL203002), the National Natural Science Foundation of China (No. 91622105).

References

- [1] K M Mantovani, K C Molgero Westrup, D S J Rm, et al. Oxidation catalyst obtained by the immobilization of layered double hydroxide/Mn (iii) porphyrin on monodispersed silica spheres. *Dalton Transactions*, 2018, 47: 3068-3073.
- [2] S Cao, J Chang, L Fang, et al., Metal nanoparticles confined in the nanospace of double-shelled hollow silica spheres for highly efficient and selective catalysis. *Chemistry of Materials*, 2016, 28: 5596-5600.
- [3] A Fong, Y Yuan, S L Ivry. Computational kinetic discrimination of ethylene polymerization mechanisms for the Phillips (Cr/SiO₂) catalyst. *ACS Catalysis*, 2015, 5: 3360-3374.
- [4] S L Zhong, L F Zhang, A W Xu. Entropically driven formation of ultralong helical mesostructured organosilica nanofibers. *Small*, 2014, 10: 888-894.
- [5] H C Wu, J H Wu, et al., Influence of sodium-modified Ni/SiO₂ catalysts on the tunable selectivity of CO₂ hydrogenation: Effect of the CH₄ selectivity, reaction pathway and mechanism on the catalytic reaction. *Journal of Colloid and Interface Science*, 2021, 586: 514-527.
- [6] E Bagheri, L Ansari, K Abnous, et al. Silica based hybrid materials for drug delivery and bioimaging. *Journal of Controlled Release*, 2018, 277: 57-76.
- [7] Z Xu, X Ma, Y E Gao, et al. Multifunctional silica nanoparticles as a promising theranostic platform for biomedical applications. *Materials chemistry frontiers*, 2017, 1: 1257-1272.
- [8] J Zhou, F Zhu, J Li, et al. Concealed body mesoporous silica nanoparticles for orally delivering indometacin with chiral recognition function. *Materials Science and Engineering: C*, 2018, 90: 314-324.
- [9] P V Naik, L H Wee, M Meledina, et al. PDMS membranes containing ZIF-coated mesoporous silica spheres for efficient ethanol recovery via pervaporation. *Journal of Materials Chemistry A*, 2016, 4: 12790-12798.
- [10] L. K. Wu, J. J. Wu, W. Y. Wu, et al., Hot corrosion behavior of electrodeposited SiO₂ coating on TiAl alloy. *Corrosion Science* 174, 108827 (2020).
- [11] X Lu, G B Zhou, J Zhang, et al. Highly Sensitive Determination of 2,4,6-Trichlorophenol by Using a Novel SiO₂@MIPIL Fluorescence Sensor with a Double Recognition Functional Monomer. *ACS sensors*, 2020, 5: 1445-1454.
- [12] K Puchnin, V Grudtsov, M Andrianova, et al. A Surface Modifier for the Production of Selectively Activated Amino Surface Groups. *Coatings*, 2019, 9: 726-740.
- [13] P Formoso, R Muzzalupo, L Tavano, et al. Nanotechnology for the environment and medicine. *Mini reviews in medicinal chemistry*, 2016, 16, 668-675.
- [14] S Huang, Z Li, L Kong, et al., Enhancing the stability of CH₃NH₃PbBr₃ quantum dots by embedding in silica spheres derived from tetramethyl orthosilicate in "waterless" toluene. *Journal of the American Chemical Society*, 2016, 138, 5749-5752.
- [15] Z Iqbal, Azhar E, E N Maraj. Performance of nano-powders SiO₂ and SiC in the flow of engine oil over a rotating disk influenced by thermal jump conditions. *Physica A: Statistical Mechanics and its Applications*, 2021, 565, 125570-125584.
- [16] L R Rowe, B S Chapman, J B Tracy, et al. Understanding and controlling the morphology of silica shells on gold nanorods. *Chemistry of Materials*, 2018, 30, 6249-6258.
- [17] B S Chapman, W C Wu, J B Tracy, et al. Heteroaggregation approach for depositing magnetite nanoparticles onto Silica-overcoated gold nanorods. *Chemistry of Materials*, 2017, 29, 10362-10368.
- [18] P Cheng, M Zheng, Y Jin, et al. Preparation and characterization of silica-doped titania photocatalyst through sol-gel method. *Materials Letters*, 2003, 57, 2989-2994.
- [19] X Lei, B Yu, H L Cong, et al. Synthesis of monodisperse silica microspheres by a modified stöber method. *Integrated Ferroelectrics*, 2014, 154, 142-146.
- [20] Q Qu, Y Min, L Zhang, et al. Silica microspheres with fibrous shells: synthesis and application in HPLC. *Analytical chemistry*, 2015, 87: 9631-9638.
- [21] H Hadoun, Z Sadaoui, N Souami, et al. Characterization of mesoporous carbon prepared from date stems by H₃PO₄ chemical activation. *Applied Surface Science*, 2013, 280: 1-7.
- [22] H Gao, Y Zhou, X Sheng, et al. Synthesis of core-shell and hollow structured dual-mesoporous silica templated by alkoxysilyl-functionalized ionic liquids and CTAB. *Materials*

- Letters, 2018, 211: 126-129.
- [23] B Peng, Y X Zong, M Z Nie, et al. Interfacial charge shielding directs the synthesis of dendritic mesoporous silica nanospheres by a dual-templating approach. *New Journal of Chemistry*, 2019, 43: 15777-15784.
- [24] Z A Qiao, L Zhang, M Guo, et al. Synthesis of mesoporous silica nanoparticles via controlled hydrolysis and condensation of silicon alkoxide. *Chemistry of Materials*, 2009, 21: 3823-3829.
- [25] X Luo, J Dong, L Zhang, et al., Preparation of silica microspheres via a semibatch sol-gel method. *Journal of Sol-Gel Science and Technology*, 2017, 81: 669-677.
- [26] Q T Pham, Z H Yao, Y T Wang, et al. Preparation and characterization of monodisperse silica nanoparticles via miniemulsion sol-gel reaction of tetraethyl orthosilicate. *Journal of Materials Science*, 2017, 52, 12706-12716.
- [27] M Meier, J Ungerer, M Klinge, et al. Synthesis of nanometric silica particles via a modified Stöber synthesis route. *Colloids and Surfaces A: Physicochemical and Engineering Aspects*, 2018 538, 559-564.